Paper No. 9

OUTER PLANETS PROBE TESTING*

J. A. Smittkamp and M. G. Grote, *McDonnell Douglas Astronautics Company, P.O. Box 516, St. Louis, Missouri 63166*
T. M. Edwards, *NASA, Ames Research Center, Moffett Field, California 94035*

ABSTRACT

An atmospheric entry Probe is being developed by NASA Ames Research Center (ARC) to conduct in situ scientific investigations of the outer planets' atmospheres. A full scale engineering Model of an MDAC-E Probe configuration, designed under NASA Contract NAS 2-7328, was fabricated by NASA ARC. Proof-of-concept test validation of the structural and thermal design is being obtained at NASA ARC. The Model has been successfully tested for shock and dynamic loading and is currently in thermal vacuum testing. It will be subjected to static testing during January 1977.

1.0 INTRODUCTION

PROBE MISSION - The mission of the Probe is to obtain in situ atmospheric measurements of the outer planets in the early 1980's. Missions to Jupiter, Saturn or Uranus are illustrated in Figure 1. Launch is followed by interplanetary cruise when the Probe is attached to the spacecraft bus. Close to the outer planet the Probe is released by the bus and functions autonomously thereafter. The Probe enters the planet's atmosphere on a ballistic trajectory, decelerates in the atmosphere, and during subsonic freefall collects and transmits data about the atmosphere.

PROBE CONFIGURATION - The Probe reference configuration is illustrated in Figure 2. External shape is a spherically blunted conical forebody with a hemispherical afterbody. The Probe weighs about 100 Kg and is 90 cm maximum diameter. Major structural components include: 1) a honeycomb sandwich primary structure aeroshell which has equipment support rings integrally machined with the inboard sandwich facesheet, 2) a honeycomb sandwich shell afterbody, and 3) attach fittings. Major thermal control components include: 1) Radioisotope Heaters, 2) the attach fittings functioning as radiators, and 3) a Multilayer Insulation blanket. During launch the Probe is held in a conical adapter which attaches the spacecraft bus to a cylindrical

*This paper is related to work performed under NASA Contract NAS 2-9027.

adapter of the launch booster.

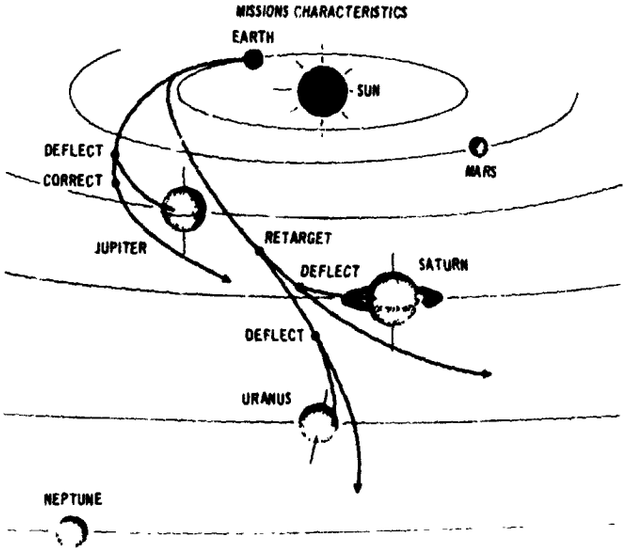

Figure 1 PROBE MISSIONS

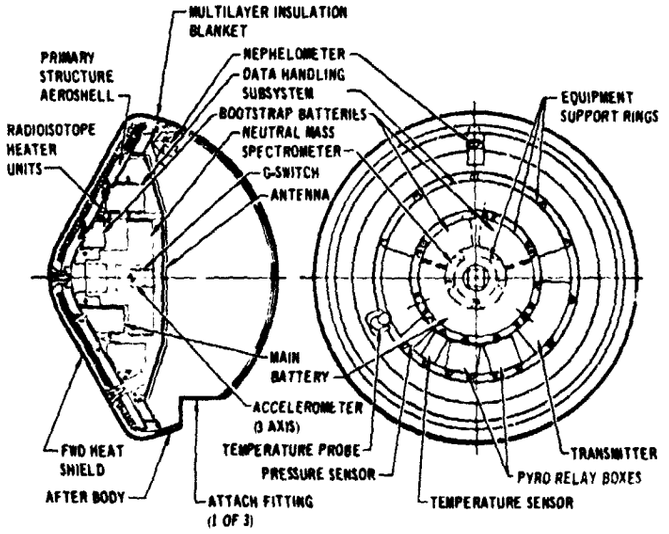

Figure 2 PROBE REFERENCE CONFIGURATION

2.0 TEST PLAN

The test plan was designed to provide a data base which would build confidence in the Probe structural and thermal design. Proof-of-concept tests which utilized a full scale Probe engineering Model as the test Model were planned and maximum use was made of NASA ARC facilities.

Mission events which are critical to the Probe structural and thermal designs were selected for test simulation. The test series and simulated flight event are presented in Figure 3. Four tests were planned; structural tests of shock, vibration, and static loads and a thermal vacuum test. The structural test series was based on a Saturn/Uranus Probe mission with a Titan III launch vehicle. Although the Shuttle is prime launch vehicle, the Titan III was chosen as being representative of launch vehicles. In addition, a Titan adapter, hardware and environments were available for testing. The thermal vacuum tests simulate a mission to any of the outer planets.

TEST	SIMULATED FLIGHT ENVIRONMENT
SHOCK	RELEASE OF PROBE FROM BOOSTER
VIBRATION	LAUNCH VEHICLE BOOST VIBRATIONS BASED ON TITAN IIIE DATA
STATIC	800 g's ATMOSPHERIC ENTRY DECELERATION
THERMAL VACUUM	INTERPLANETARY CRUISE

Figure 3 TEST PLAN SUMMARY

The shock test subjected the Model to shock environment resulting from simulated separation from the launch vehicle.

The vibration test subjected the Model to the dynamic environment of launch.

The static test will simulate quasi-static loading expected during an 800 gg deceleration during planet atmospheric entry.

The thermal vacuum tests are simulating the deep space interplanetary cruise and the approach cruise portion of a mission.

3.0 TEST MODEL

A full scale engineering Model of the Probe was fabricated by NASA ARC to serve as the test Model. The Model was fabricated per engineering drawings of a MDAC-E Probe designed in a preliminary definition study for NASA-ARC. Completed Model hardware

is illustrated in Figures 4 to 6. An external view of the partially assembled Model resting on a machining fixture is given in Figure 4. The figure shows one of the recessed attach fittings. Figure 5 shows the Multilayer Insulation blanket wrapped around the Model. Simulated equipment was also fabricated and is shown in Figure 6 installed on the equipment support rings of the aeroshell. The simulated equipment approximated the

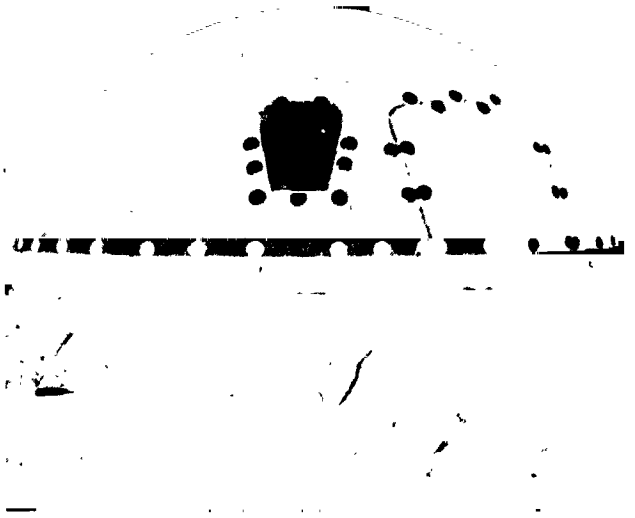

Figure 4 [illegible]E ENGINEERING MODEL – PARTIALLY ASSEMBLED

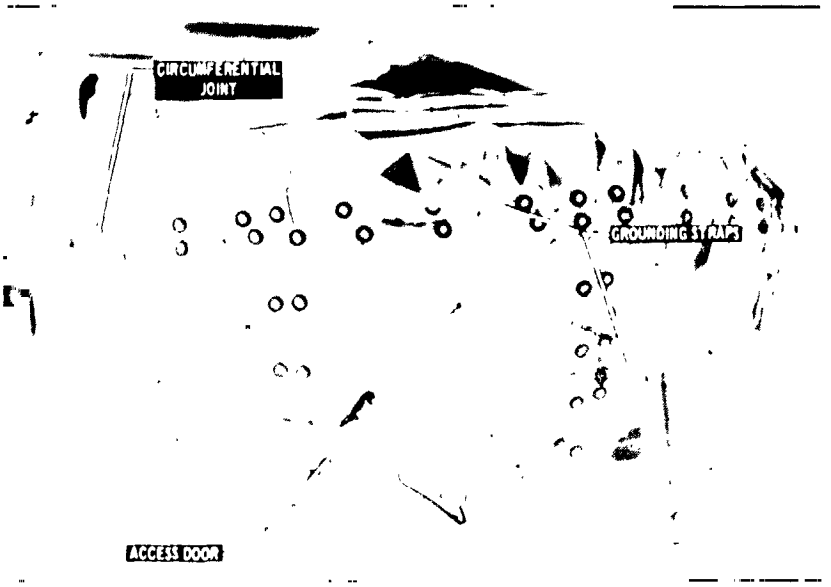

Figure 5 MULTILAYER INSULATION BLANKET

shape, size, weight and attachment pattern of anticipated equipment. Element heaters were installed in the simulated equipment to simulate equipment heat output during thermal vacuum tests. Figure 6 also shows the three attach fittings which connect the Probe to the conical adapter.

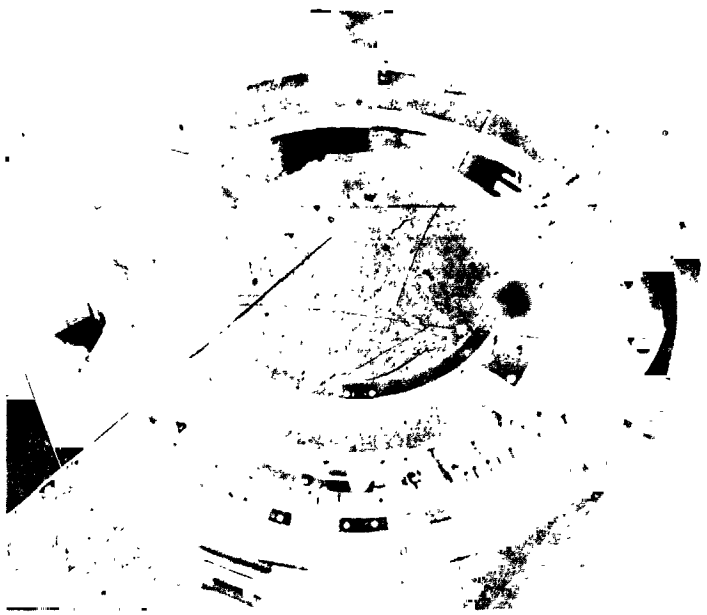

Figure 6 SIMULATED EQUIPMENT IN AEROSHELL

4.0 STRUCTURAL TESTS

CONFIGURATION - The structural subsystem of the Probe is schematically illustrated in Figure 7. The primary structure consists of a honeycomb sandwich aeroshell having a fiberglass outer facesheet and an aluminum inner facesheet. Four equipment support rings are integrally machined with the aluminum facesheet. The aeroshell acts as a decelerator, protects the equipment during 800 gg's ballistic deceleration and provides continuous support for the forward heat shield. The rings distribute concentrated equipment inertia loads into the aeroshell. Three attach fittings located 120 degrees apart in the afterbody attach the Probe to the conical adapter.

SHOCK TESTS

Stage separation of the Probe and conical adapter from the last stage of the launch vehicle would be accomplished by the release of a V-band clamp ring. The clamp ring disengages when two diagonally opposite preload bolts are cut by pyro actuated bolt cutters. The resulting shock may be critical on the ball

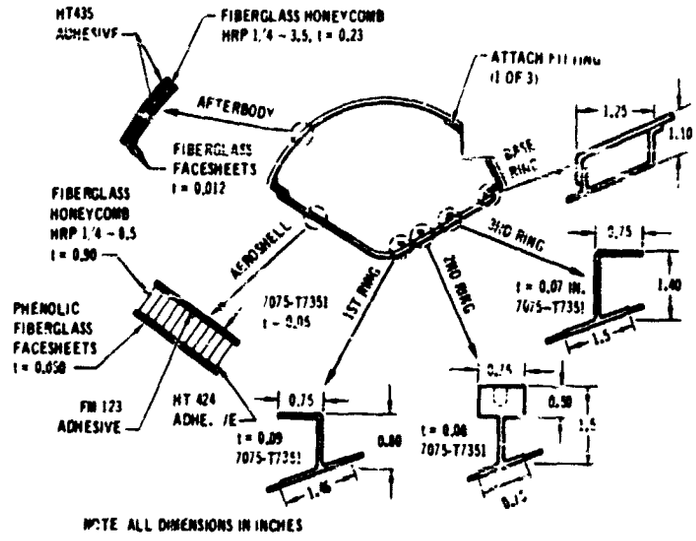

Figure 7 STRUCTURAL CONFIGURATION

lock bolts which attach the Probe to the conical adapter at the attach fittings. (The ball lock bolts utilize pyro generated pressure to self-actuate, allowing the Probe to separate from the conical adapter, and can be sensitive to shock loads.) The primary objective of the shock test was to determine the effect of shock on the operation of the ball lock bolts. Two shock tests were conducted and provided test data for the extreme positions of bolt cutters relative to the ball lock bolts.

The shock test setup is schematically illustrated in Figure 8. The Model with simulated equipment was mounted in the conical adapter. This subassembly was then attached to the cylindrical adapter of the Titan III with a V-band clamp ring.

A closeup photograph of the test hardware is shown in Figure 9. The photograph shows the conical adapter, the cylindrical adapter, the V-band clamp ring, one of the pyro actuated bolt cutters and one of the three ball lock bolts. Two 3-axis accelerometers are shown, one directly above the bolt cutter and the other by the ball lock bolt. Also shown are air pressure lines connected to the ball lock bolt. These lines were used to provide air pressure to actuate the bolts in lieu of pyrotechnic pressurization.

The first test was conducted with one of the bolt cutters aligned directly beneath a ball lock bolt as illustrated in Figure 9. The bolt cutters were actuated and the V-band clamp ring disengaged. Accelerations at all of the gages were continuously recorded. After all structural response to the shock had died

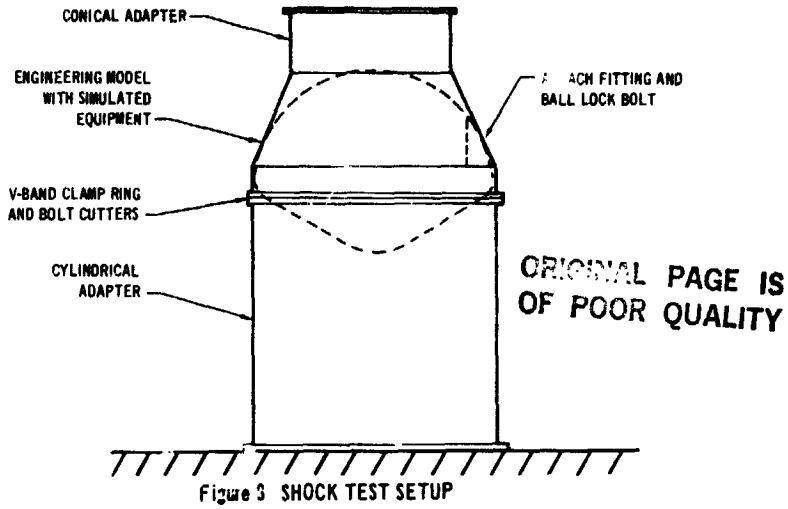

Figure 3 SHOCK TEST SETUP

Figure 9 PHOTOGRAPH OF SHOCK TEST HARDWARE

down, a Model/conical adapter separation test was conducted and the three ball lock bolts operated successfully allowing separation.

The Model and conical adapter were then rotated so that both bolt cutters were 30° from the nearest ball lock bolts and the second test was conducted.

Maximum acceleration of 1920 g's was recorded at an attach fitting during the second test. Maximum acceleration at the ball lock bolts was 800 g's recorded during the first test. Accelerations at the equipment support ring were very small for both tests. These accelerations are acceptable.

In addition to supplying the acceleration data, these tests demonstrated proof-of-concept:

(1) The two pyro bolt cutters actuated successfully allowing the V-band clamp ring to properly disengage.

(2) Following each shock test, the three ball lock bolts were successfully actuated and the Model separated from the conical adapter.

(3) No structural failures occurred and the structure significantly attenuates the shock loads and significantly reduces shock requirements for equipment.

VIBRATION TESTS

The launch dynamic environment may be critical for the attach fittings which transmit launch accelerations and environments to the Probe. The primary objective of the vibration test was to determine the dynamic response of the attach fittings to simulated launch environment. A secondary objective was to obtain qualitative information of the dynamic characteristics of the structural design.

The longitudinal vibration test setup was similar to that for the shock tests except that aircraft bolts were used in lieu of the ball lock bolts and V-band clamp ring pretension bolts. The setup also used a LING A300B shaker table, a head expander to accommodate the large diameter cylindrical adapter and team tables to ensure that only longitudinal (vertical) table motion occurred.

Instrumentation consisted of eight accelerometers attached to the Model to provide qualitative information of structure dynamic characteristics.

A photograph of the longitudinal vibration test setup is shown in Figure 10. From top to bottom are shown the conical adapter, cylindrical adapter, head expander and LING A300B shaker table. One of the team tables to ensure vertical table motion is also shown.

Six vibration tests were conducted; a sinusoidal and a random along each of the Model orthogonal axis. The longitudinal axis was tested first with the setup shown in Figure 10. The shaker table was then rotated to a horizontal position, the

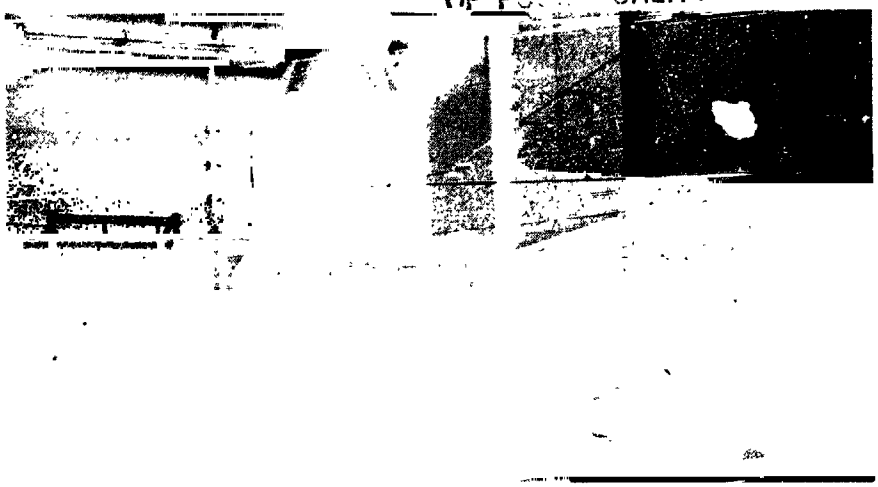

Figure 10 PHOTOGRAPH OF VIBRATION TEST HARDWARE

vertical team tables were removed and vibration tests of the two lateral axes of the Model were conducted. Input environment was controlled at the head expander. The input environments were those given in Figure 11 with one exception. Due to equipment limitations (primarily shaker output capability vs mass of the test specimen and fixtures)the overall level obtained for the longitudinal axis was only 3.16g instead of 8.16g equivalent for random vibration.

The structure appears to have good dynamic characteristics. No major problems were found. The only significant amplifications (greater than 10) of the input environments occurred at

VIBRATION AXIS	SWEEP RATE	FREQUENCY (Hz)	ACCELERATION (g's 0-PEAK)
LONGITUDINAL	1 OCTAVE/MIN	5–12	3.0
		12–50	3.0
		50–200	2.25
BOTH LATERAL	1 OCTAVE/MIN	5–10	1.95
		10 22	1.95
		22–200	1.50

SINUSOIDAL TEST VIBRATION SCHEDULE

VIBRATION AXIS	TEST DURATION (MIN. EACH AXIS)	FREQUENCY (Hz)	POWER SPECTRAL DENSITY (PSD) LEVEL (g^2 Hz)
ALL 3 AXIS	4	20–100	0.056 AT 100 Hz INCREASE BY 6 dB PER OCTAVE FROM 20–100 Hz
		100–1000	0.056
		1000–2000	0.056 AT 1000 Hz WITH ROLL OFF OF 12 dB PER OCTAVE FROM 1000-2000 Hz

RANDOM VIBRATION TEST SPECTRUM AND DURATION

Figure 11 VIBRATION TEST LEVELS

the simulated relay box and simulated antenna. A maximum amplification of 34 at 12 Hz occurred at the relay box during lateral sinusoidal vibration and an amplification of 18 at 86 Hz occurred at the antenna during the longitudinal axis sinusoidal vibration. Close attention to the designs of the actual relay box and antenna will be required to reduce these amplifications.

During testing, local structural failures occurred in the afterbody near the cutouts for two of the three attach fittings. The failures were minor and were not detected until all six tests were completed. It is not known which test initiated the failures. One of the failures is shown in the photograph of Figure 12. The afterbody honeycomb sandwich facesheets separated from the core near the core reinforcements. The failures are primarily attributed to the cantilever design of the attach fittings. Modification of the attach fitting design was recommended to provide better load paths.

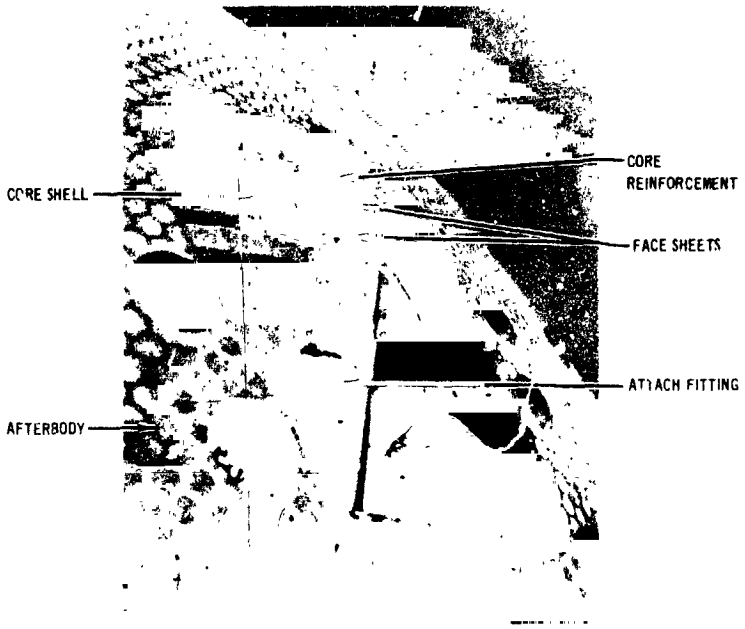

Figure 12 AFTERBODY LOCAL FAILURE - VIBRATION TEST

STATIC TESTS (These tests will be conducted during January 1977)

The aeroshell supports the equipment under 800 g_E's inertia loading balanced by the forebody aerodynamic pressure during planetary entry. Primary objective of the static tests is to determine strength of the aeroshell under this loading.

The static test setup is schematically illustrated in

Figure 13. Only the aeroshell of the Model will be tested and will be mechanically loaded in a specially designed static test fixture as illustrated in Figure 13. A photograph of the partially assembled static test fixture is presented in Figure 14. The fixture was designed and fabricated by NASA ARC and will simulate loading of the aeroshell expected during atmospheric entry deceleration of up to 800 g_E's.

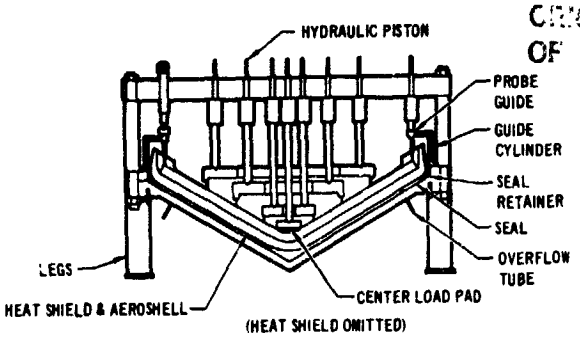

Figure 13 STATIC TEST SETUP

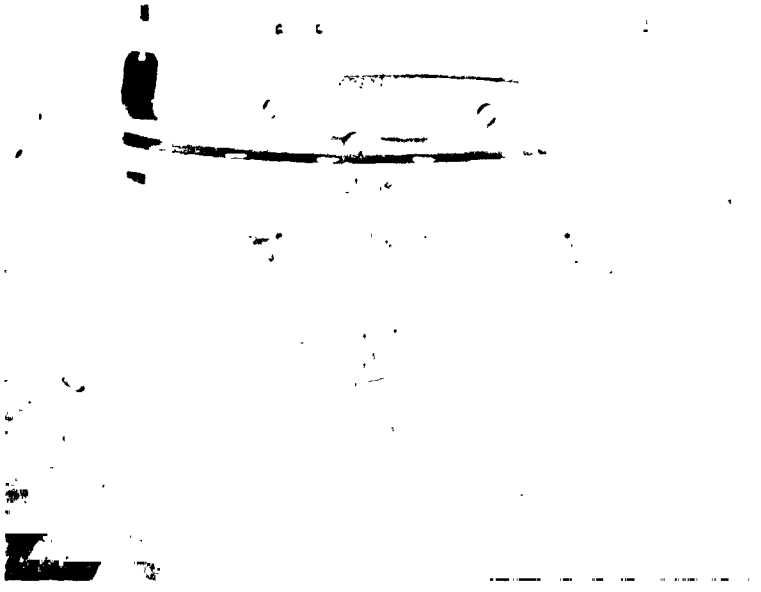

Figure 14 ARC STATIC TEST FIXTURE

The fixture will apply hydrostatic pressure to the forward side of the aeroshell to simulate atmospheric deceleration pressure. Loads to balance the pressure will be applied by hydraulic pistons to the aeroshell equipment support rings to simulate

inertia loads of the equipment. The piston loads will be transmitted to the rings by stiff load distribution plates. Radial deflection isolation of the plates from the rings is provided for.

5.0 THERMAL VACUUM TESTS

CONFIGURATION - The baseline configuration of the Probe thermal control subsystem is shown in Figure 15. During interplanetary cruise, the Probe is attached to the spacecraft's conical adapter and the temperature within the Probe will be controlled between 253°K and 273°K by adjusting the temperature of the attachment fittings via radiators and commandable heaters located on the conical adapter. This temperature range will insure long battery life.

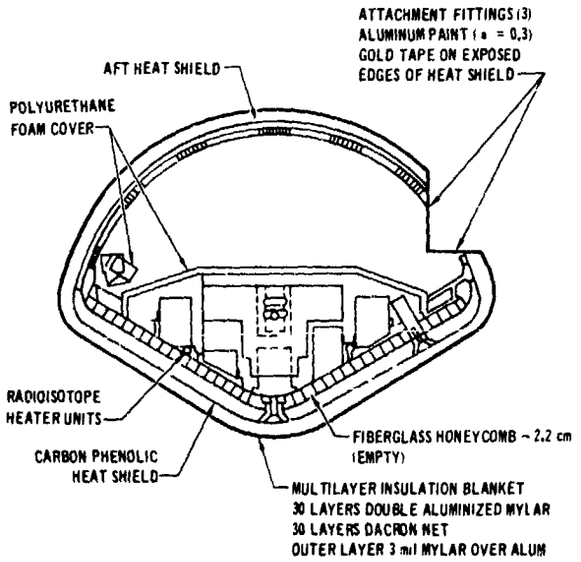

Figure 15 THERMAL CONTROL SUBSYSTEM REFERENCE DESIGN

Depending on the planet, the Probe is separated from the spacecraft between 21 and 56 days prior to entry. During this approach cruise phase, the Probe's internal temperature will be maintained by a balance between the heat loss through the Multilayer Insulation (MLI) blanket and the attachment fittings with the heat generated by the Radioisotope Heating Units (RHU's). Prior to entry, all equipment within the Probe are at essentially the same temperature and will be between 263°K and 283°K. Temperatures higher than 283°K will begin to limit the mission time during the hot atmospheric descent. The minimum activation temperature of the battery is 278°K, but a heater is located on the battery which can be activated prior to entry to raise the battery temperature by as much as 15°K if necessary, thus establishing the 263°K lower limit. The MLI blanket consists of 30

layers of double aluminized mylar and 30 layers of dacron net. The outer layer is a 3 mil mylar over aluminum sheet, and the entire blanket is held together with nylon buttons. There are two joints in the blankets; one around the circumference of the maximum diameter and one around the access door. Figure 5 (Section 3.0) shows the completed blanket installed on the Model. The attach fittings are painted with a low emissivity aluminum paint and the exposed edges of the heat shield near the attach fittings will be covered with low emissivity tape to prevent low temperature exposure on the edge of the heat shield.

TEST PLAN - The purpose of the thermal vacuum test was to verify the passive thermal control concept and to measure the thermal performance characteristics of the Probe Model and the Probe to conical adapter interface. These data will include such items as insulation properties of the flight configured blanket, heat flow paths within the Model and the transient characteristics. The test plan shown in Figure 16 consists of eight runs. The first four runs simulate the approach cruise phase of the flight with the third run being a transient run to simulate the pre-entry power profile as shown in Figure 17. Only the first four runs are addressed in this paper.

RUN NO.	SIMULATION	TYPE	CONDITIONS
1	APPROACH CRUISE	STEADY STATE	RHU = 8 WATTS
2	APPROACH CRUISE	STEADY STATE	RHU = 10 WATTS
3	APPROACH CRUISE	TRANSIENT	PREENTRY POWER PROFILE
4	APPROACH CRUISE	STEADY STATE	RHU = 12 WATTS
5	INTERPLANETARY CRUISE	STEADY STATE	RHU = 10 WATTS ADAPTER TEMP ~ 294°K
6	INTERPLANETARY CRUISE	STEADY STATE	RHU = 10 WATTS ADAPTER TEMP = 244°K
7	INTERPLANETARY CRUISE	STEADY STATE	RHU = TBD WATTS ADAPTER TEMP = 244°K
8	INTERPLANETARY CRUISE	TRANSIENT	EQUIPMENT CHECKOUT POWER PROFILE

Figure 16 TEST RUN MATRIX

TEST METHODS - Several differences exist between the test configuration and the reference design, Figure 15. The facilities did not have the capability for projecting a simulated solar input of sufficient diameter to cover the Model, and thus solar simulation was not used. Secondly, a higher emissivity aluminum paint (ε = 0.43) was used in place of the Finch type (ε = 0.30) aluminum paint. For the test, the RHU heat dissipation was simulated with heaters installed in typical RHU containers.

To maintain the internal Probe temperatures at specified levels with relatively few RHU's, the Probe must be extensively insulated. This yields a long time constant for the Model which presents problems in reaching steady state conditions within a

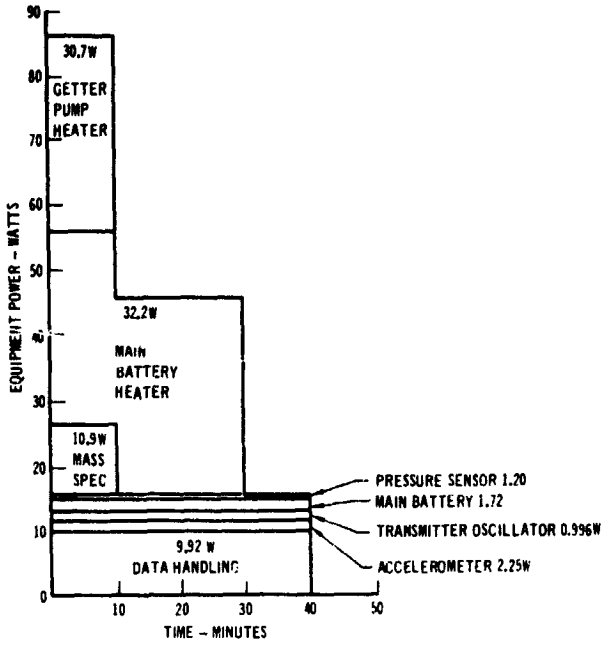

Figure 17 PREENTRY POWER PROFILE

short period of time. Thus, methods were evolved using an analytic simulation to accelerate the attainment of steady state conditions.

The first problem was how and at what level to initialize the Model temperature. The uncertainty in the MLI performance would yield uncertainties in the steady state temperatures. To accelerate the cooldown, all of the heaters are turned off and the Model is allowed to cool until it reaches an estimated value of the steady state temperature (TSS). At this time, the simulated RHU heaters are turned on and the first run is started. To estimate TSS, an existing analytic simulation of the Model was used. The cooldown characteristics of the Model were estimated by running a zero load transient and an eight watt steady state analytic simulation for two values of the MLI conductance that should bracket the performance. For each curve there is a characteristic slope and a corresponding steady state value (TSS) for the initial eight watt case. Thus, the TSS can be estimated from the slope of the cooldown curve, and was calculated as follows:

$$T_{SS8} = 352 - 9.6\ (T_{\tau} - T_{\tau-1\ day}) \qquad (1)$$

where

T_τ = Temperature at present time

$T_{\tau-1\ day}$ = Temperature 1 day earlier

T_{SS8} = Estimated steady state value for 8 watt load

Procedures were also developed to accelerate the run during the course of the run and to derive an applicable steady state criteria. Again, the analytic simulation was used to determine steady state values and expected transient responses during the course of the run. Figure 18 shows a plot of $\frac{dT}{d\tau}$ vs $T - T_{SS}$, and the slope of this curve represents the reciprocal of the time constant of the Model. From this plot the following correlating equation was derived:

$$TSS = T_\tau + 14.2\ (T_\tau - T_{\tau-1\ day}) \qquad (2)$$

The first use of this equation was in establishing the steady state criteria. A change of temperature of 1°K per day will only insure that we are within about 14°K of the final answer and thus a much smaller temperature change must be used as the criteria. To measure these small temperature changes a platinum resistance thermometer (PRT) was included in the instrumentation, and a steady state criteria of 0.1°K change per day was established. During the course of a run, the steady state temperature can also be estimated from Equation (2). To change the temperature, additional heaters can be turned on to raise the temperature, or the simulated RHU heaters can be turned off to accelerate the cooldown.

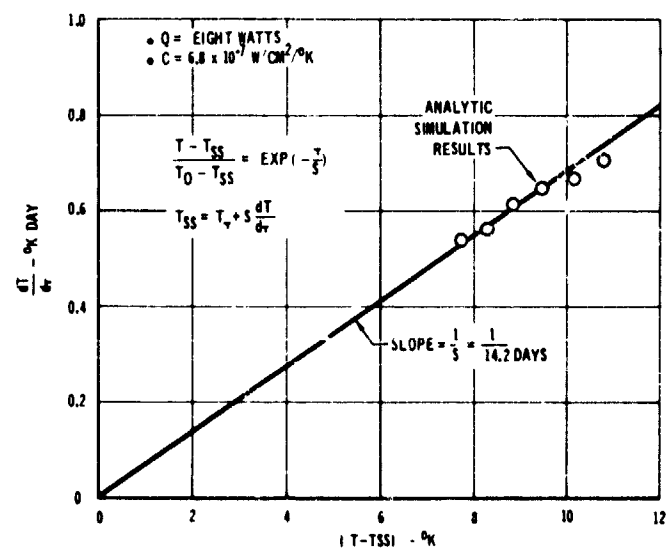

Figure 18 PROBE TIME CONSTANT

To obtain the necessary data, the Model was instrumented with 50 thermocouples (T/C) and one PRT. Each component was instrumented with one or more T/C, and one of the attach fittings was instrumented with six T/C to determine the heat flow paths near the attach fittings. T/C's are also located on the external side of the blanket to help determine insulation properties. A total of 13 heater sets are located within the Model. All of the T/C's and heater wires are brought out in one wire bundle. Since this wire bundle is fairly large (>2 cm dia.) it could be a significant heat leak. To prevent this, the wire bundle was insulated with a MLI wrap and a heater block was located in the bundle about 30 cm from the Model. This heater was tied into a variable voltage controller which was driven by a difference temperature measurement between the heater and the Model. The heater input is varied to maintain a temperature differential of less than $\pm 1°K$, which results in a heat leak of less than 0.1 watt.

TEST RESULTS - The first run was initialized at about 257°K, and the eight watt simulated RHU load was turned on. Figure 19 presents a plot of the bootstrap battery temperature as a function of time. By the middle of day 285, it was apparent that the Model temperature was too low. Using Equation (2) the steady state value was estimated to be 267°K and heaters were turned on to raise the temperature. The temperature initially rose rapidly to a spike and then fell after the heaters were turned off as the localized heating was gradually absorbed into the forward heat shield. Thus, monitoring one of the internal temperature sensors is not a good indication of the finalized temperature, but the total heat input is a good indicator. The resultant temperature rise after the heating spike was about 0.053°K per watt-hr of applied heat. This one temperature level change was all that was necessary to reach stability. The calculated time constant, though, was about 7.0 days as compared to the 14.2 days of Equation (2). With the 7 day time constant, the first test would have taken 23 days to complete if started at room temperature as compared to the 7 days actual test time using the accelerated methods. Based on the results of the first run, the approximate additional watt-hrs (QA) to boost the Model to steady state conditions could be calculated as:

$$QA = \frac{7\ (T_{\tau} - T_{\tau-1})}{0.053} \qquad (3)$$

Figure 20 presents the plot of the bootstrap battery for run No. 2. At the beginning of the run, the temperature was initially raised to the expected level. As with Run No. 1, only one additional temperature adjustment was necessary. Figure 21 presents the steady state temperatures for Run No. 2, and shows that all the equipment temperatures are within a few degrees of each other. Run No. 4 had to be terminated early because of a water cooling failure in the diffusion pump, but the results are

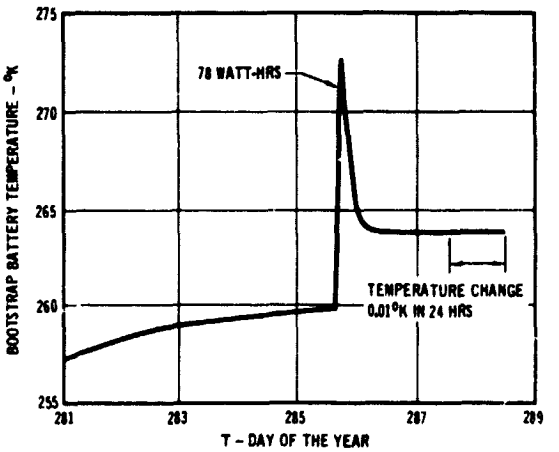

Figure 19 TEST RUN NO. 1 – 8 WATTS

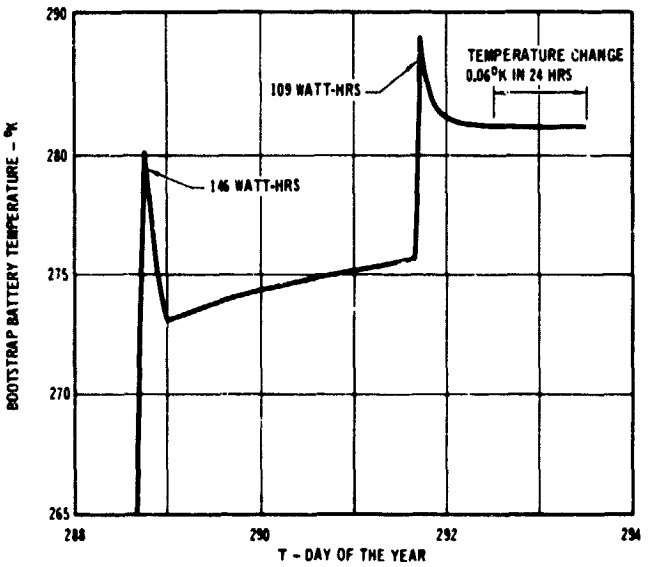

Figure 20 TEST RUN NO. 2 – 10 WATTS

within 2°K of the true steady state results. Figure 22 presents the steady state battery temperature tests results compared to the analytic predictions. Although the temperatures are in the expected range, the slope of the test data is smaller than the analytic prediction. Further analytic work will be necessary to resolve this discrepancy. At the completion of Run No. 2, the pre-entry power profile was run, and the results are presented in Figure 23. As is shown, the battery heater does raise the battery temperature by the required 15°K.

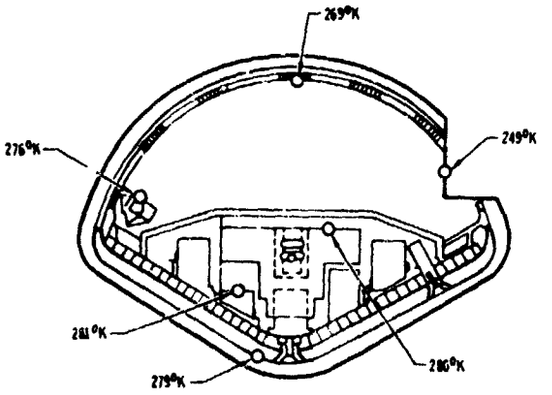

Figure 21 STEADY STATE TEST RESULTS
RUN NO. 2 – 10 WATTS

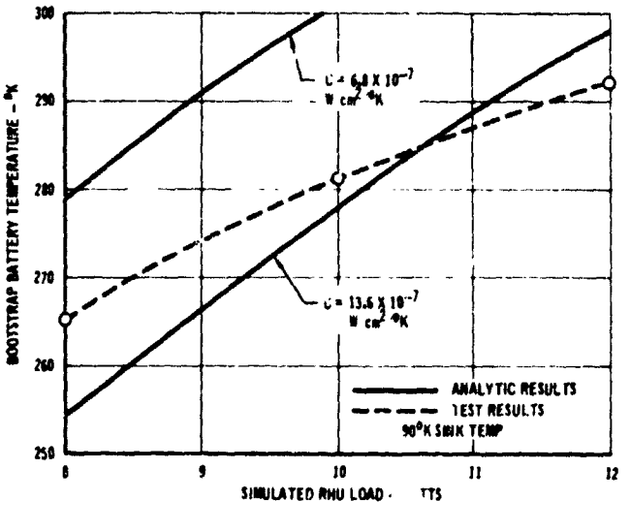

Figure 22 APPROACH CRUISE SIMULATION STEADY STATE TEST RESULTS

TEST CONCLUSIONS - As tested, the Probe Model requires less than nine 1 watt RHU's to maintain the desired 273°K nominal temperature level. Since the simulation did not include solar input and had a higher emissivity paint on the attach fittings than the reference design, the actual requirement will be less. Thus, the concept of controlling the Probe passively with a relatively few number of RHU's has been successfully demonstrated. Further analytic work will be required to correlate the analytic simulation to the test results in order to perform trade studies to determine the final configuration with a high degree of confidence. Although the preliminary correlating Equations (1) and

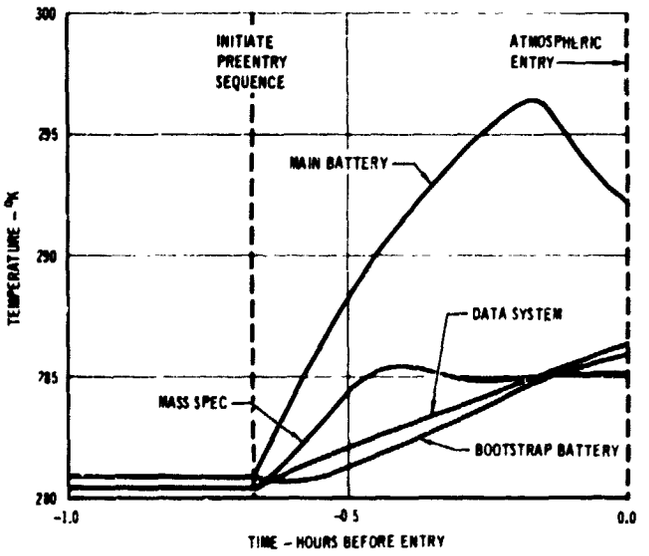

Figure 23 PREENTRY TRANSIENT RUN NO. 3

(2) did not exactly match the actual Model characteristics, the procedures for accelerating the testing did significantly decrease the testing time.

6.0 SUMMARY

Proof-of-concept tests are being conducted on a full scale engineering Model of the Probe. The tests simulate critical conditions expected during the Probe mission. Shock and vibration tests are completed and indicate that the structural concept is basically sound. Thermal vacuum testing successfully demonstrated the passive control concept and verified methods of accelerating the testing. Future static testing will further validate the structural concept.